Adsorption (2012) 18:403–415
DOI 10.1007/s10450-012-9424-0

Flux response technology applied in zero length column diffusivity measurements

Ayodeji Sasegbon · Klaus Hellgardt

Received: 4 June 2012 / Accepted: 17 September 2012 / Published online: 10 October 2012

Abstract Flux Response Technology (FRT) has been successfully adapted as an *in situ* perturbation technique in dynamic gas sorption measurements to extract hydrocarbon diffusion coefficients in alumina/$CeZrO_x$ washcoats of cordierite monoliths. FRT works by measuring minuscule changes in flowrate between two gas streams for any gaseous process involving a change in volume ($\delta V/\delta t$). Ad- and desorption transients, which can be collected during the same experimental run have been analysed using the zero length column (ZLC) method to study propane diffusivity within an alumina/$CeZrO_x$ washcoat as a function of temperature. Extracted diffusivities and activation energies compare favourably with literature data.

Keywords Flux response technology · In situ · Diffusion · ZLC · Perturbation

1 Introduction

Diffusion within porous materials has been widely studied by scientists and industry for its useful and important applications in molecular separation, heterogeneous catalysis, membrane technology, fuel cells, soil mechanics and petroleum engineering. The importance of accurately being able to model diffusivity is highlighted extensively in many catalytic combustion applications associated with power generation and pollution control (Heck et al. 2010; Tomašić 2007; Gonzo and Gottifredi 2010; James et al. 2003; Boger et al. 2004; Chen et al. 2004). The well known automotive catalytic converter makes use of a catalytic monolith reactor in a 'honeycomb' configuration to oxidise carbon monoxide and unburned hydrocarbons while reducing oxides of nitrogen. These reactors possess several obvious advantages over traditional reactors packed with catalyst particles—lower pressure drop, uniform flow distributions, uniform residence times and less hot-spot formation (Armenisea et al. 2010; Heck et al. 2001). Metals and ceramic materials such as cordierite are commonly used as monolith materials. Cordierite is a material chosen due to its high melting point of over 1000 °C, resistance to oxidation and resistance to thermal shock, which is required to meet the severe operating conditions in automotive exhausts (Brito et al. 2005; Ciambelli et al. 2010). Metallic monoliths have been used since the early 1990s and offer advantages when compared to cordierite such as higher frontal areas approaching 90 % which provides higher geometric surface areas while offering low resistance to flow. However, due to their metallic nature, the expansion coefficient is much greater than ceramics, thereby requiring special bonding techniques to produce an adherent washcoat (Heck et al. 2001). The washcoat found typically on monolithic ceramic substrates contain the active catalyst layer of fine precious metal particles for example, platinum and rhodium in the case of the automotive industry (Plummer et al. 2003).

The ability to model the performance of monolith supported catalysts is a crucial tool required by manufacturers in order to rapidly explore alternative system designs, lower development costs and increase speed of production. To this effect, understanding the diffusion that occurs within the washcoat and substrate material which strongly affects reactor performance is essential in the design of monolith supported catalysts (Zhang et al. 2004; Koci et al. 2007; More et al. 2006). With these factors in mind, it must be ac-

A. Sasegbon · K. Hellgardt (✉)
Department of Chemical Engineering and Chemical Technology, Imperial College London, South Kensington Campus, London SW7 2AZ, UK
e-mail: k.hellgardt@imperial.ac.uk

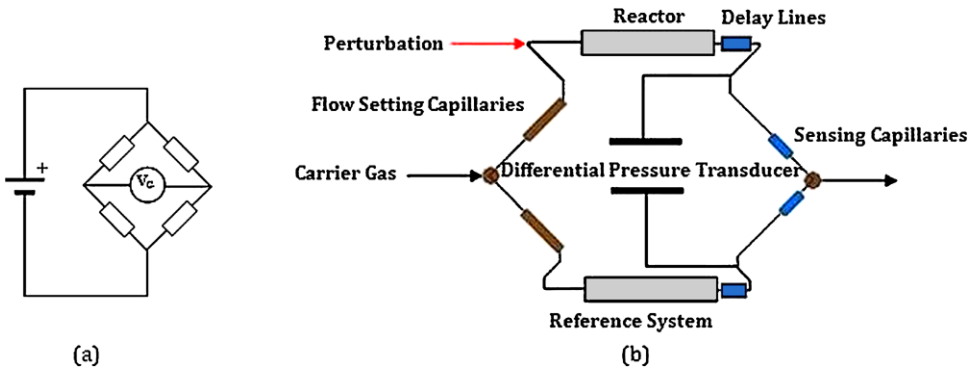

Fig. 1 Schematic of the experimental configuration for Flux Response Technology: (**a**) Electrical Wheatstone bridge assembly, (**b**) Pneumatic Wheatstone bridge assembly

knowledged that the diffusion coefficients reported in literature for microporous materials often vary with differences as large as five orders of magnitude being reported for different techniques (Kärger 2012). The discrepancies between different techniques have since been resolved and can be traced to the different length scales over which diffusion is measured (Chmelik et al. 2011). Measured diffusivities were found to be smaller when the path length covered in the measurement is large (macro-measurements) suggesting the intrusion of extra-crystalline transport resistances in addition to the diffusional resistance of the pore system (Ruthven 2001; Chmelik et al. 2011; García-Sánchez et al. 2012). The purpose of this paper is to measure propane diffusivity in the washcoat of monolith samples using Flux Response Technology (FRT) and to show that this method can be used to compare and contrast with other micro and macroporous techniques in one experiment by analysing the adsorption and desorption transients in the FRT profile. In previous studies (Buffham et al. 2000; Richardson et al. 2004; Palmer et al. 2011), we have shown the versatility of the FRT method in measuring adsorption, reaction and desorption *in situ* in the reactor. By applying the Zero Length Column (ZLC) method to analyse the sorption curves generated by the FRT system, the rate of diffusion in the washcoat is calculated.

2 Theory

2.1 Fundamentals of FRT

Flux Response Technology (FRT) is a powerful and versatile gas *in-situ* technique that is able to analyse miniscule transient flow rates in the order of 10^{-2} µl/min. The technique is based on capillary viscometry and can be used to measure minuscule changes in flowrate between two gas streams for potentially any gaseous process involving a change in molar hold-up ($\delta N/\delta t$) (Buffham et al. 1986a, 1986b; Mason 1998; Russell et al. 2002, 2003; Palmer et al. 2011). FRT functions analogous to an electrical Wheatstone bridge assembly whereby gas molecules represent electrons and flow capillaries represent resistors. A schematic of the Wheatstone bridge assembly is illustrated in Fig. 1. One side of the bridge, referred to as the *system side*, can be perturbed by pressure, concentration and temperature. The other side of the bridge, parallel to the system side is the *reference side* and is setup to replicate the experimental configuration of the system side. An imbalance in the pneumatic Wheatstone bridge between the system and reference sides caused by a perturbation is measured by a differential pressure transducer (DPT) as a voltage difference and can be used to carry out very sensitive differential measurements for a range of processes.

During operation, the flow setting and flow sensing capillaries cause a fixed pressure difference between the system and the reference side of the Wheatstone bridge, thereby resulting in a constant flowrate through the entire apparatus. The upstream (flow setting) capillaries cause a 99 % pressure drop, which determine the carrier gas flowrate. Having the flowrates the same on both sides of the bridge gives rise to a null response for the apparatus with an initial pressure difference (p_0) which is detected by the DPT. Once a perturbation of probe molecules is introduced to the apparatus, the Wheatstone bridge assembly becomes imbalanced by the additional flow and the DPT detects a new pressure (p_1) within milliseconds—a near instantaneous response time due to the low pneumatic resistance of the pneumatic network. The virtually incompressible nature of the gas causes it to behave like a piston and pressure changes travel to the sensing DPT at the speed of sound of the carrier gas. Because the change in pressure Δp caused by the probe molecules perturbation is small compared to the total pressure p of the apparatus and, with little error, the gas can be assumed ideal at room temperature and just above atmospheric pressure, the perturbation signal can be linearised.

Since the perturbation signal reaches the DPT within some milliseconds (based on the length scale of the equipment), a signal is observed well before the perturbation reaches the outlet of the apparatus. Therefore, FRT falls into the category of *in situ* techniques. Ultimately, it is the DPT, which limits the response time of the apparatus to 10 milliseconds.

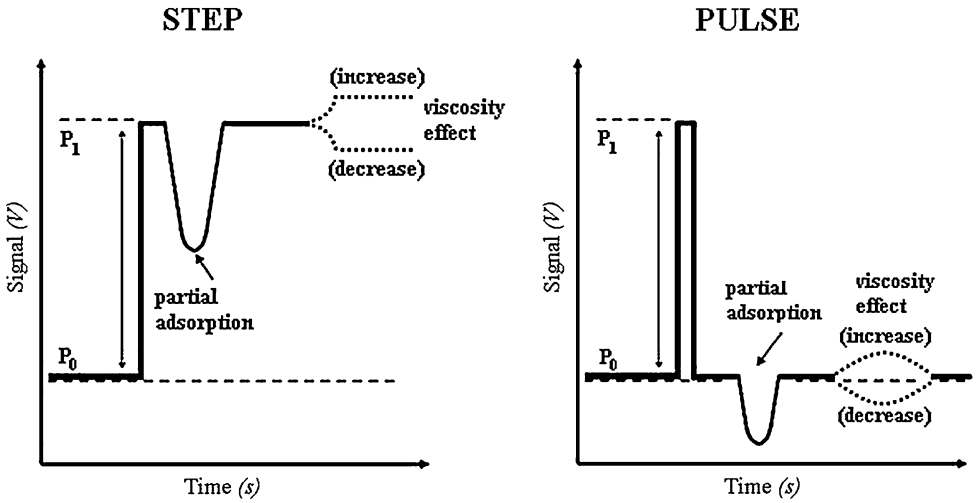

Fig. 2 Typical flux response profiles for pulse and step experiments

Downstream of the upstream capillary chokes are the *delay lines*. The delay lines play a vital role in separating out the individual responses/phenomena during an experimental run by extending the path length of the signal to the DPT. These lines are pieces of empty tubing, typically several metres of $\frac{1}{4}''$ PFA tubing or a custom-made delay box that provide the important and powerful feature of allowing FRT to act as a combined flowrate and composition detector. Elucidating this point further, the addition or removal of a perturbation causes a near instantaneous pressure response, whereas the pressure responses from composition effects can be postponed as these only occur when the composition front reaches the sensing capillaries. Figure 2 presents examples of typical FRT profiles for single component adsorption. The integral of the pressure response (the area underneath the peaks) has been shown to be directly proportional to the amount of probe molecules in the perturbation adsorbed onto the catalyst surface (Richardson et al. 2008). Therefore, FRT can be considered as a perfect molar flow meter.

Pulse and step experiments constitute the two key experimental methods used for FRT experiments. Pulse experiments involve the injection of tiny quantities of probe molecules for a limited period and they are highly suited to titration experiments. Whereas, step experiments entail the continuous injection of probe molecules until the system achieves a steady state or quasi equilibrium. Step experiments can be used to study the dynamic cyclic behaviour of a sample. Although both types of experiments reveal similar information, data extraction from step experiments is less complicated. Nevertheless, regardless of the experimental approach, the quantities of probe molecules that are injected into the system can be tightly controlled via the concentration and duration of the pulse/step.

The governing equations used to extract information from the flux response profile are developed by understanding the flow through the sensing capillary. Theoretically, the flow can be described by the Hagen-Poiseuille Law for laminar flow. Assuming the flow through the sensing capillary is laminar, viscous and incompressible, the change in pressure (p_z) with distance z for the flow of fluid through a section of tube of the sensing capillary is given by,

$$\frac{dp_z}{dz} = -K_c \mu Q \tag{1}$$

where Q is the volumetric flowrate, μ is the viscosity and K_c is a constant dependant on the characteristics of the tube. For an ideal gas,

$$Q = \frac{MRT}{p_z} \tag{2}$$

M is the molar flowrate of gas, p_z is the pressure at distance z, T is the absolute temperature and R is the gas constant. By substituting for Q in (1) with (2), the longitudinal pressure gradient can be expressed as

$$p_z \frac{dp_z}{dz} = -K_c \mu MRT \tag{3}$$

The viscosity of a gas is dependant primarily on temperature. At low pressure, it is considered to be independent of pressure which makes μ a constant in (3) (the sensing capillaries are kept at a constant temperature). Integrating along the whole length of the capillary tube gives the following equation;

$$p^2 - P_{BPR}^2 = 2K\mu MRT \tag{4}$$

where $K = K_c L$, L is the length of the capillary tube, p is the pressure at the inlet of the capillary and P_{BPR} is the outlet pressure (Mason et al. 1998).

2.2 FRT for the measurement of gas sorption

The FRT system was setup to perform *in-situ* measurements of propane sorption in monolith samples of cordierite

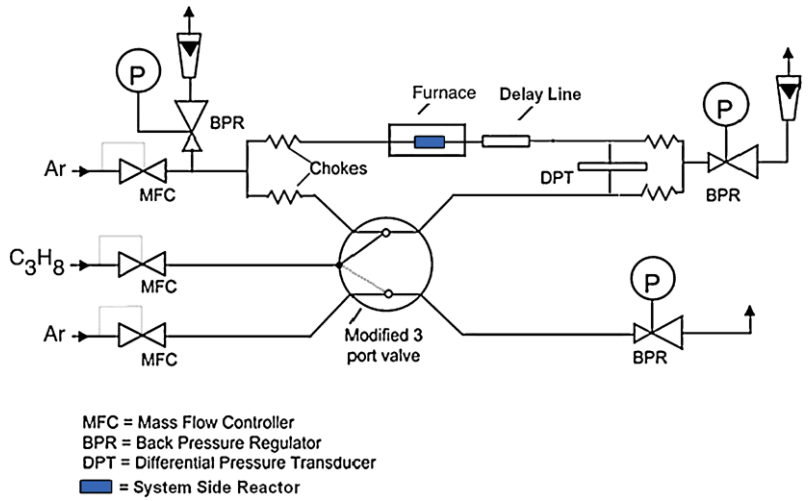

Fig. 3 Schematic of the FRT experimental setup for the measurement of propane sorption across a temperature range between 25 °C to 100 °C

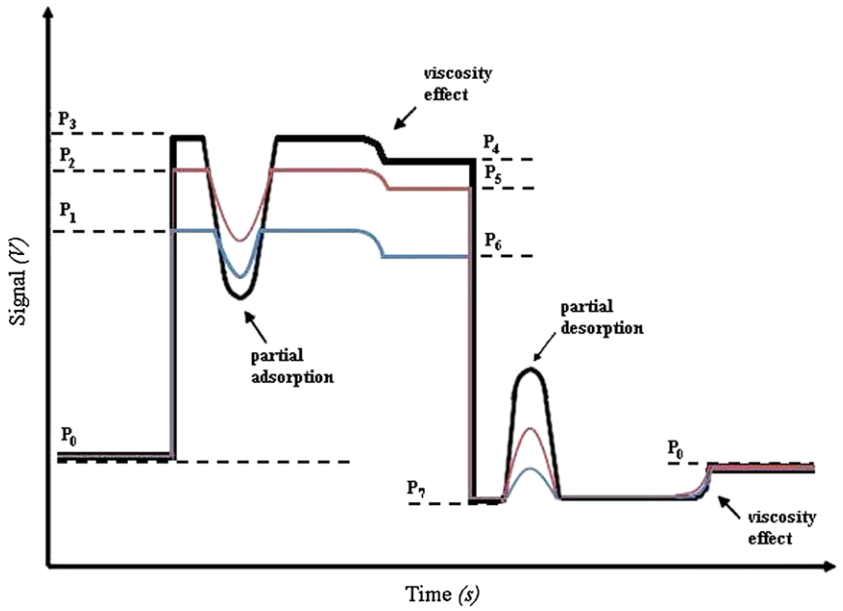

Fig. 4 Schematic of expected flux response profile for C_3H_8 sorption under isothermal conditions for varying molar fractions of C_3H_8 perturbation gas in Ar carrier gas i.e. P_1/P_0, P_2/P_0, P_3/P_0

with an alumina/$CeZrO_x$ washcoat over a range of temperatures, 25–100 °C. The experimental configuration involves the integration of a temperature programmable furnace into the Wheatstone bridge assembly. The temperature programmable furnace houses the system reactor, a quartz tube containing a fixed bed of the test sample in a well defined geometry. Depending on whether the system reactor causes a pressure drop, a reference reactor may be used on the reference side of the Wheatstone bridge assembly to shift the baseline of the experiment. A schematic of the experimental configuration and the expected flux response profile are presented in Figs. 3 and 4.

In order to calculate the diffusivity within the washcoat of the monolith samples, it is necessary to apply the ZLC method to analyse the FRT generated sorption curves. This method was introduced in 1988 (Eic and Ruthven 1988) and has since been widely used to study both micropore and macropore diffusion (Eic and Ruthven 1988, 1989; Silva 1996; Cavalcante et al. 1997; Ruthven and Brandani 2000; Gunadi and Brandani 2006; Guimarães et al. 2010). The ZLC method of measuring diffusivity depends on following the desorption of sorbate from a previously equilibrated sample of adsorbent into an inert carrier stream. In this study, the experimental adsorption curves were also analysed to evaluate the diffusion of sorbate into post-calcined monolith samples. The experimental sorption curves were interpreted according to the original simplified model of Eic and Ruthven (1988) where the analysis utilizes the long time region of the decay curve.

Table 1 Material Cordierite monolith with alumina/$CeZrO_x$ washcoat

Material	S_{BET} (m^2/g)	$S_{Langmuir}$ (m^2/g)	Pore size ($\times 10^{-9}$ m)
Sample 1	22.73	31.61	9.11
Sample 2	22.52	31.23	9.03
Sample 3	23.69	32.82	9.36
Sample 4	25.44	35.28	9.17

2.3 Mathematical model for ZLC analysis

The ZLC method is based on the following assumptions: spherical adsorbent particles, Fickian diffusion, linear sorption isotherm, perfect mixing through the cell, isothermal conditions, high flowrate of the gas stream and neglect of fluid phase hold-up. From these assumptions, the response curve is given by (Crank 1979):

$$\frac{c}{c_0} = 2L \sum_{n=1}^{\infty} \frac{\exp(-\frac{\beta_n^2 Dt}{r^2})}{[\beta_n^2 + L(L-1)]} \tag{5}$$

where β_n is given by the roots of;

$$\beta_n \cot \beta_n + L - 1 = 0 \tag{6}$$

and

$$L = \frac{1}{3} \frac{Fr^2}{K V_s D} \tag{7}$$

In these equations, c represents the concentration at any time t, c_0 is the initial concentration, F signifies the purge flowrate, V_s is the crystal volume in the ZLC cell, K represents the dimensionless Henry law constant, D is the diffusion coefficient, r is the particle radius, while L and β_n are dimensionless parameters. In the long time region (the tail of the respective sorption curves) (5) reduce to simple exponential decay curves as only the first term of the summation is significant:

$$\frac{c}{c_0} = \frac{2L}{[\beta_1^2 + L(L-1)]} \exp\left(-\frac{\beta_1^2 Dt}{r^2}\right) \tag{8}$$

A plot of $\ln(c/c_0)$ vs. t should give a linear asymptote in the long time region from which the slop and intercept can be used to calculate parameters D and L.

3 Materials and methods

3.1 Propane sorption across a temperature range of 25 °C to 100 °C to determine diffusivity and activation energies

Four samples of cordierite monoliths with varying alumina/$CeZrO_x$ washcoats were supplied by a manufacturer. The material characterisation of the samples was carried out using a Micromeritics Tristar 3000 surface analyser and the data are compiled in Table 1.

The cordierite samples were crushed and sieved to size a fraction of 425–850 µm. Preparation of the samples before starting an experiment was achieved by heating in a high purity gas stream of argon (99.99 %, BOC) from room temperature to 400 °C overnight. In order to regenerate the samples after each temperature cycle, they had to be heated at 400 °C for 30 min. Typically, approximately 0.186–0.190 g of each monolith was used in each experiment. The reactor was a 4 mm i.d. quartz tube with the test sample held in place by two plugs of quartz wool. The sorbate used in the experiment was propane (98 %, Sigma Aldrich) and argon (99.99 %, BOC) was used as the carrier gas. The monolith samples were studied over the range of 25–100 °C. The test samples were investigated with propane at 0.5 molar fraction running through the system side of the apparatus during perturbations.

The differential pressure between the system and reference flows just upstream of the measuring resistances was measured using a differential pressure transducer (Furness Controls, model FCO 44), interfaced to a data logging PC. Delay lines, which were lengths of empty 1/4″ o.d. PFA tubing, were employed to delay the time at which the composition (and hence viscosity) of the gas passing through the measuring resistance changed.

4 Results and discussion

4.1 Propane sorption for diffusivity measurements between 25 °C to 100 °C

Shown in Fig. 5 is an example of the flux response profile for sample 3. Figure 5(a) shows an expanded view of the first dynamic cycle and highlights the partial desorption effect. Figure 5(b) presents the entire FRT experiment by showing the three dynamic cycles. As expected, a strong correlation between the expected flux response profile detailed earlier and the experimental flux response profile shown in Fig. 5 is apparent. The key effects are the propane partial adsorption

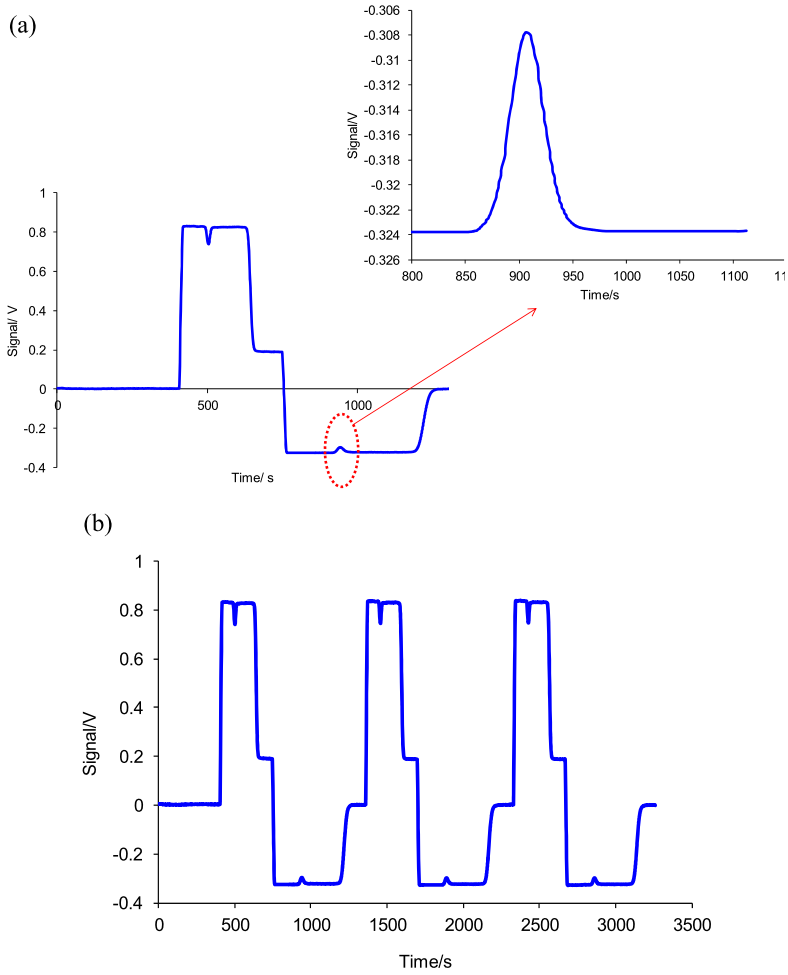

Fig. 5 Flux response profile for Sample 3 at C_3H_8 mole fraction of 0.5: (**a**) first sorption cycle, (**b**) complete experiment showing three sorption cycles

peak; the viscosity effect caused by the propane perturbation into argon carrier gas; propane partial desorption peak; and the viscosity effect caused by the composition of the gas changing from a propane/argon mixture to purely argon carrier gas.

For the investigation of diffusivities within the washcoats of the cordierite samples, it was necessary to analyse the concentration of the adsorbable species (C_3H_8 in this instance) in the effluent stream in order to apply the ZLC analysis. As stated earlier, the measuring element within the FRT apparatus is an extremely sensitive DPT capable of measuring flowrate changes of the order of 10^{-2} µl/min. The differential pressures measured by the DPT are directly proportional to the amount of probe molecules ad/desorbed onto or from the surface of the adsorbent (Richardson et al. 2008). As such, with reasonable accuracy, the responses by the DPT in the flux response profiles can be considered linear and directly proportional to the quantity of C_3H_8 released into the effluent stream.

Figure 5(a) presents the partial adsorption and desorption curves that are required for the analysis of propane diffusivity. The analysis of the FRT partial sorption curve required the response curves to be normalised to the initial concentration by using the following equation (Brandani 2002):

$$\frac{c(t)}{c_0} = \frac{\sigma(t) - \sigma_{\text{inf}}}{\sigma_0 - \sigma_{\text{inf}}} \tag{9}$$

where, σ_0 is the value of the FRT signal at time zero and σ_{inf} is the value of the FRT signal at the respective sorption completion times. The data acquisition from the DataShuttle/USB 54 system (Adept scientific) linked to a desktop computer was started at the beginning of the experiment, recording all the FRT responses to the C_3H_8 perturbation. Consequently, in order to clearly evaluate σ_0, the time scale from the data acquisition had to be shifted back by t_0 seconds for each sorption curve. It was also necessary to invert the FRT profile along the x-axis at the region correspondent to the partial adsorption effect to be able to analyse its decay.

Figure 6 represents the normalised decay curve from the FRT generated desorption curve for ZLC analysis. It is worth noting the form of the FRT profile displayed above. Ruthven et. al have shown the concentration profile for a sample which is subjected to a step change in surface concentration where the slope is curved, increasing from high to

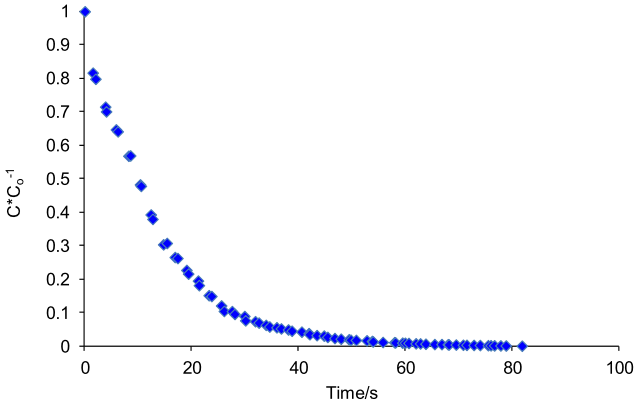

Fig. 6 Experimental FRT-ZLC desorption curve (C_3H_8 mole fraction, 0.5) of Sample 3 at 25 °C

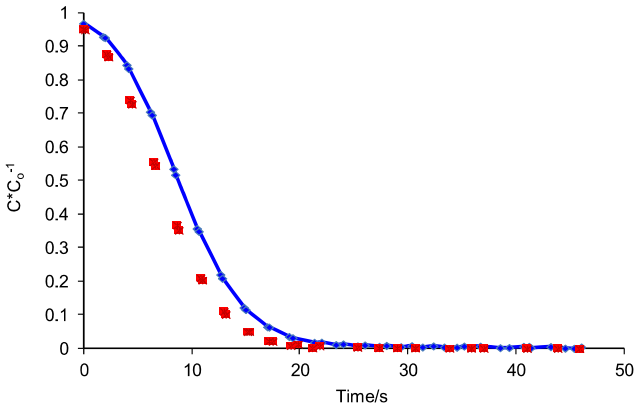

Fig. 7 Comparison of the FRT-ZLC curves measured for FRT system in the presence (♦), and absence (■) of Sample 3 at 25 °C (C_3H_8 mole fraction, 0.5)

low concentration, much akin to that shown in Fig. 6 is characteristic of a system where surface resistance controls the diffusivity within the sample (Ruthven et al. 2010). The initial step drop in concentration is signature in samples where surface resistance control dominates.

Once this curve was generated, it was necessary to account for apparatus effects influencing the measured signal response such as dispersion, dead volume and adsorption on tube walls. When the perturbation gas is switched in during the experiment, the dispersion of the probe molecules through the tubes connected to the switch-in valve can have a significant role on data analysis. Such an effect can dominate the signal response as is shown in the Fig. 7 and needs to be corrected for using a blank run. The trade-off between systematic errors brought about through pressure drops within the FRT apparatus and dispersion effects through the tubes of the apparatus had to be limited during the building of the FRT system and as such, such apparatus effects would have to be accounted for during data analysis. By comparing the curves of the FRT setup in the presence and absence of the test sample, it was possible to evaluate the full extent of the dispersion effect for identical system conditions. Figure 7 shows the comparison of response with the test sample and the corresponding blank.

The reason for performing the blank experiments as a comparative tool stemmed from preliminary experiments where the generated ZLC models for the FRT desorption curves fitted the long time region of the curves accurately but seriously underpredicted the initial concentrations. As is shown in Fig. 7, the concentration ratio falls to approximately zero in roughly 17 s when no sample is present while it takes approximately 21 s when a sample is present. This result negates the possibility of the underprediction being due simply to a slow system response time. Both experiments show a pronounced tail from 21 s which indicates the likely cause is due to an apparatus effect associated with dispersion through the system as stated earlier. From the developed double exponential (Loos 2000), it was possible to limit the influence of this dispersion by simply subtracting the difference between the models generated for the blank experiment from those with the sample present to allow the accurate application of the ZLC equations. The exponential function in (10) was used to model the dispersion effect where the characteristic times, τ_1 and τ_2 are the characteristic times for the dispersion effect, I and I_0 are the intensity at any time t and the maximum intensity at the start of the decay, respectively, and t_0 is an offset depending on whether the curve starts at time = 0.

$$I = I_0 e^{\left(\frac{t_0 - t}{\tau_1}\right)} + (1 - I_0) e^{\left(\frac{t_0 - t}{\tau_2}\right)} \tag{10}$$

The results of the blank experiments were also able to yield valuable information relative to the working of the FRT system. Adapting the ZLC technique in FRT system provided the additional capability of measuring fast diffusion processes by taking advantage of the very sensitive DPT. The FRT system responds to any substance whose extent of sorption differs from that of the carrier, thereby making it possible to measure flow rate changes instantaneously as the capillary detection system behaves as though it has no volume (Buffham et al. 1993). The arrangement of the DPT and matched capillaries provide the system with a resolution of one part in ten thousand, however, the response time of the system can be reduced further still at the expense of the sensitivity and vice-versa (Buffham et al. 1986a, 1986b). The internal diameter of the capillaries which control the pneumatic resistances are a compromise between these conflicting system requirements whereby the gas species are conveyed as quickly as possible to the packed bed, minimising dispersion within the system without restricting the sensitivity of the DPT to perform differential measurements. The system runs with and without an adsorbent present are showcased in Fig. 7 and are normalised relative to their initial concentrations. Each run was performed to indicate

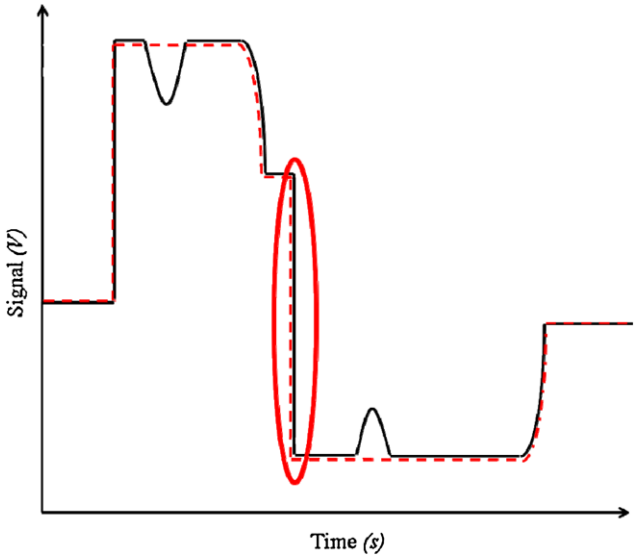

Fig. 8 Schematic flux response profile for case with and without adsorbent present

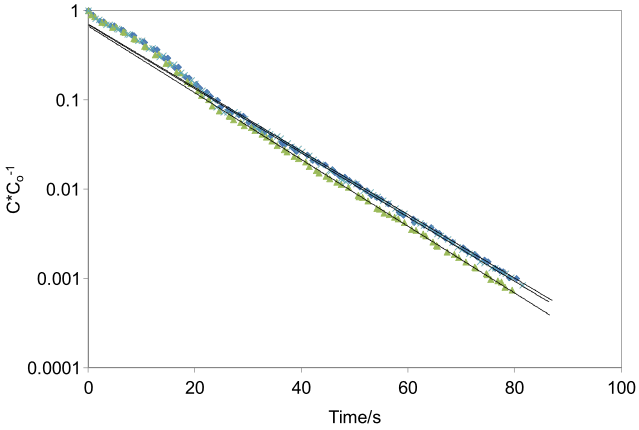

Fig. 9 Experimental FRT-ZLC desorption curve for Sample 3 at 40 °C (C_3H_8 mole fraction, 0.5) for all three cycles (1st cycle—*blue rhomb*, 2nd cycle—*green triangle*, 3rd cycle—×) showing the long time asymptote approach

the level of dispersion within the system which was subsequently subtracted from the generated sorption curves to account for this dispersion. The slow response time can be explained by considering the size of the perturbation stream which was set at 0.5 mole fraction.

Shown in Fig. 8 above is a schematic flux response profile for the present study. The black line represents the expected flux response profile with an adsorbent present while the dashed red line represents the blank system. Evaluating the dispersion in the system was carried out by comparing the profiles at the circled region—the point at which the perturbation stream is switched out leaving the carrier gas to flow on its own through the reactor. As can be noticed from the graph, a large step change is exhibited and attributed to the perturbation stream. Measurements acquired by the data acquisition software across this region where the blank response was evaluated do show a prolonged signal response due to the large pressure change but this is expected as the signal simply follows the path length through the system of the loss in pressure from the perturbation stream being switched out.

The effective time constant of this system can therefore be evaluated by considering the blank response time of the propane probe. From Fig. 7, it is clear that equilibrium is achieved after approximately 17 s, but already between 0–5 s, the average of the data collected is equal to 72 % of the equilibrium value. By programming the data logger to record acquisitions at shorter time intervals, the transient responses would be recorded much more accurately. Analysing the decay of the response with the effects of thermal noise and dispersion that are specific to the FRT system, it was possible to estimate the maximum measurable value of D/R^2 by fitting an exponential curve to the response. This yielded a value of 0.6 s^{-1}.

Having taken the dispersion effect into account, it was then possible to evaluate the ZLC parameters, D and L from (5). By generating a plot of $\ln(c/c_0)$ against t, it was possible to calculate these parameters by using the slope and intercept of the linear asymptote in the long time region. This is known as the long time (LT) analysis in ZLC studies (Brandani 2002):

The slope and intercept of the semilogarithmic plot of c/c_0 vs. t are given, according to (8) by:

$$S = \beta_1^2 D/r^2; \qquad I = 2L/\left[\beta_1^2 + L(L-1)\right] \tag{11}$$

By combining the intercept and transcendental equation (6), the root of transcendental equation β_1 was found using (12).

$$\beta_1 - \cot\beta_1 + \beta_1 \cot^2\beta_1 + \frac{2\beta_1 \cot\beta_1 - 2}{\beta_1 Intercept} = 0;$$
$$\beta_1 \in (0, \pi) \tag{12}$$

Equation (11) was solved analytically using Maple software, from which the value of the time constant, D/r^2 and hence the diffusion coefficient could be solved.

Presented in Fig. 9 is the log-scale approach of the long time asymptote for all 3 cycles of sample 3 at 40 °C. It is clear that the asymptotes of these response curves are similar. This is in accordance with (7), where for a given temperature, L should be proportional to the purge flowrate. As the purge flowrate at each cycle was the same, it was expected that the generated asymptotes would be similar. One of the advantages of the ZLC experimental method is that for any particular system, the validity of the basic assumptions under the experimental conditions can be verified directly by a series of simple experiments. In performing the three cycles

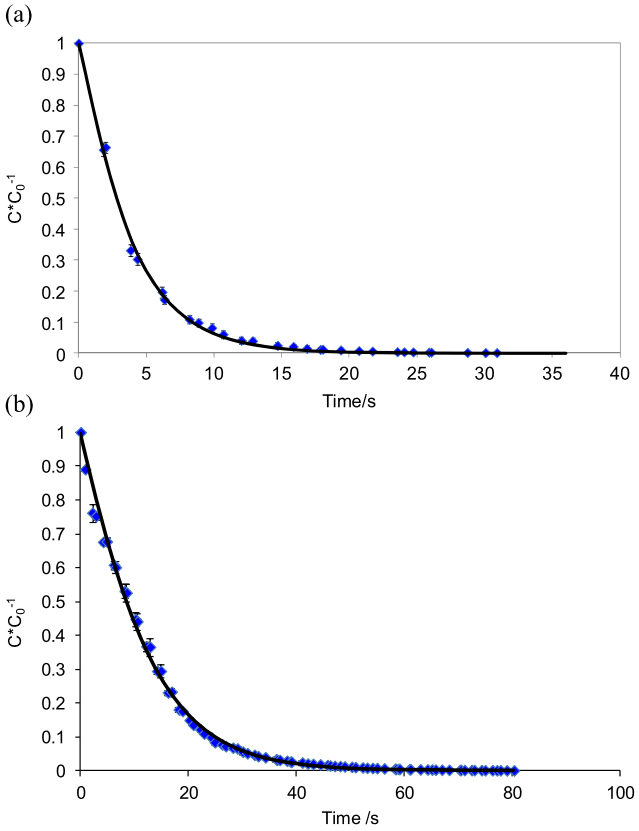

Fig. 10 FRT experimental (*points*) and fitted (*solid line*) curves for Sample 3: (**a**) adsorption transient, (**b**) desorption transient, using propane (mole fraction, 0.5) at 40 °C

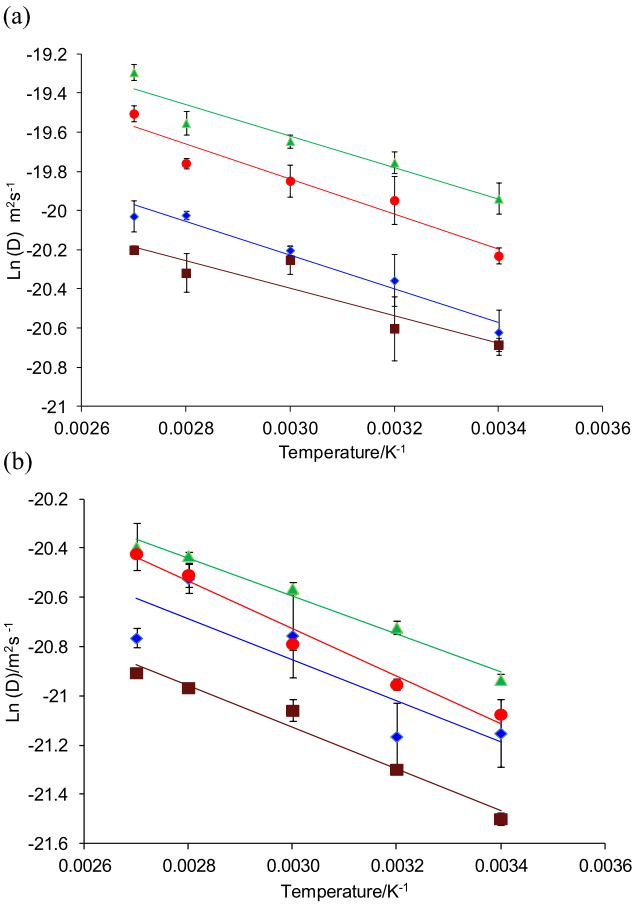

Fig. 11 FRT diffusion coefficients at temperatures between 25–100 °C for (**a**) averaged adsorption cycles, (**b**) averaged desorption cycles, showing Sample 1 (■), Sample 2 (♦), Sample 3 (▲), and Sample 4 (●)

required for the complete FRT-ZLC experiment and comparing their asymptotes, a test for the validity of the ZLC assumptions was inadvertently carried out. Other researchers have performed similar tests by varying the flowrate of the purge gas and comparing the long time asymptotes. In such cases, the generated asymptotes would be expected to be parallel from one another (Gobin 2006; Karge et al. 2008; Guimarães et al. 2010).

From the evaluated ZLC parameters, it was possible to construct the FRT-ZLC plots with the experimental sorption curves fitted with the ZLC model. Figure 10 is an example of the experimental curves with their appropriate models.

It is clear from Fig. 10 that a good agreement exists between both experimental adsorption and desorption curves and the LT model for ZLC diffusion, thereby confirming the validity of the experimental method and analysis. Graphs of the diffusion coefficients for each of the monolith samples were plotted against temperature to compare both ad and desorption transients and to analyse the respective activation energies of diffusion.

Figure 11 summarises the variation of the diffusion coefficients of the samples with respect to temperature. The first observation that can be deduced from the graphs show that the diffusion coefficients from the adsorption transient in part (a) are larger than those from the desorption transient in part (b). However, both show a similar linear trend for the variation of the diffusivity coefficients with respect to increasing temperature, as expected. By taking the average of the adsorption and desorption values, a good estimate of the diffusivity coefficients of the samples can be evaluated and is shown in Table 2.

The activation energies and pre-exponential factors for diffusion were determined from the Arrhenius-plots given in Fig. 11, in accordance with (13).

$$D_{eff} = D^o e^{\frac{-E_A}{RT}} \tag{13}$$

The reported values in Table 3 show that the activation energies of diffusion for the adsorption transient were lower than those of the desorption transient. This is an expected result as the activation energies of the adsorption process are nearly always smaller than those of desorption (Ranke and Joseph 2002).

Table 2 Diffusivity coefficients of averaged FRT response transients

Sample	Temperature (K)	D ($m^2\ s^{-1}$)
Sample 1	298	7.5×10^{-10}
	313	8.5×10^{-10}
	333	1.2×10^{-9}
	353	1.1×10^{-9}
	373	1.3×10^{-9}
Sample 2	298	8.8×10^{-10}
	313	1.0×10^{-9}
	333	1.3×10^{-9}
	353	1.6×10^{-9}
	373	1.5×10^{-9}
Sample 3	298	1.5×10^{-9}
	313	1.8×10^{-9}
	333	2.1×10^{-9}
	353	2.3×10^{-9}
	373	2.8×10^{-9}
Sample 4	298	1.2×10^{-9}
	313	1.5×10^{-9}
	333	1.7×10^{-9}
	353	1.9×10^{-9}
	373	2.4×10^{-9}

Table 4 shows the derived diffusivity values with the evaluated ZLC model parameter L as well as the Henry constants for adsorption and desorption present.

Table 4 exhibits the temperature dependence of the evaluated Henry's constants for each sample. It can be observed that the Henry's constants are inversely proportional to temperature as is expected. The Henry's constants show that the affinity of propane to the cordierite samples is as follows: Sample 3 > Sample 4 > Sample 1 > Sample 2. Table 5 compares evaluated Henry's constants for Sample 3 with literature values.

The evaluated Henry's constants in Table 5 once again show the dependence on temperature for similar adsorbates. The values of the Henry's constants also show a marked decrease with increasing adsorbate chain length (Fig. 12).

Table 6 gives the activation energies for diffusion determined by other techniques to compare with this study. Large variations between the measured values are observed (Eic and Ruthven 1989; Sun et al. 1996a, 1996b; Granato et al. 2010) dependant on whether the technique is microscopic or macroscopic in nature. The microscopic techniques generally result in high diffusivities and low activation energies for diffusion. Conversely, the macroscopic techniques generally have high activation energies for diffusion and diffusivity values as much as five orders of magnitude lower when compared with the microscopic techniques.

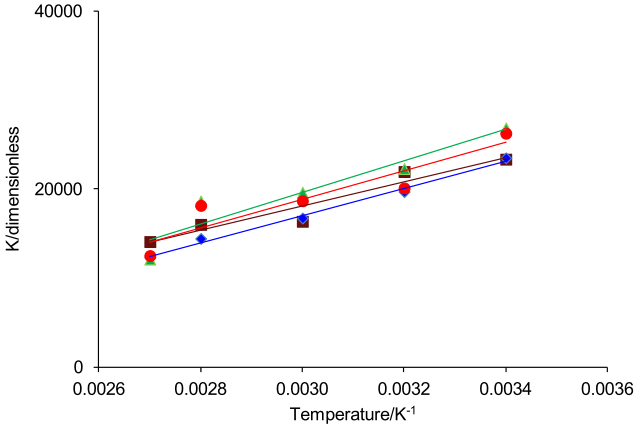

Fig. 12 Henry constants at temperatures between 25–100 °C showing temperature dependence of Sample 1 (■), Sample 2 (♦), Sample 3 (▲), and Sample 4 (●)

It is reassuring to observe that the calculated activation energy for propane diffusion in alumina/$CeZrO_x$ (extracted from the Arrhenius plot of diffusivities measured at different temperatures, Fig. 10) compares well to that predicted by Granato et al. (2010) based on theoretical molecular dynamics simulations of propane diffusion in 13X, and pulse field gradient nuclear magnetic resonance (PFG-NMR) data by Schwartz et al. (1995). The results also compare well to the values of Sun et al. (1996a, 1996b) who employed a Wicke-Kallenbach type method using a zeolite membrane and report diffusivities of propane in silicalite in the temperature range between 30 to 70 °C as 4–6 × 10^{-10} m^2/s.

Brandani et al. (1995) observed that propane diffusivity in 13X is much smaller when measured with the ZLC approach as compared to PFG-NMR. Banasa et al. (2005) suggest that this may be due to the PFG-NMR technique returning intra-crystalline diffusivities whereas ZLC experiments result in the observation of combined diffusion and desorption processes. By observing the dispersion corrected decay curves of the adsorption transient, FRT was able to measure the transport kinetics of the washcoat material without interfering concurrent desorption. This appears to yield satisfactory results as the dispersion corrected adsorption parameters of diffusivity compare particularly well with other macroscopic techniques (Karger and Ruthven 1992). Another advantage of the technique is that FRT measures the diffusivity into the washcoats of the monoliths at the instance of propane reaching the bed of the material thereby reducing the error margins suffered by other chromatographic techniques in which dispersion through the column affects the accuracy of such results.

5 Conclusions

FRT has been successfully adapted for the *in situ* measurement of zero length column diffusion in $CeZrO_x$ wash-

Table 3 Comparison of activation energy (E_A) parameters of FRT transients

Material	Pre-exponential factor ($m^2\ s^{-1}$)		Activation energy ($kJ\ mol^{-1}$)	
	FRT adsorption	FRT desorption	FRT adsorption	FRT desorption
Sample 1	1.1×10^{-8}	8.3×10^{-9}	6 ± 0.6	7 ± 0.4
Sample 2	1.4×10^{-8}	9.5×10^{-9}	6 ± 2.2	7 ± 1.6
Sample 3	2.6×10^{-8}	1.0×10^{-8}	6 ± 1.0	6 ± 0.8
Sample 4	3.2×10^{-8}	1.7×10^{-8}	7 ± 1.1	8 ± 0.1

Table 4 Diffusivity and model parameters for FRT-ZLC experiments

Sample	Temperature (K)	D ($m^2\ s^{-1}$) (ads)	L (–)	K (–)
Sample 1	298	1.0×10^{-9}	4.78	23 355.38
	313	1.1×10^{-9}	4.68	21 958.50
	333	1.6×10^{-9}	4.42	16 374.04
	353	1.5×10^{-9}	4.83	16 024.85
	373	1.7×10^{-9}	4.88	14 096.21
Sample 2	298	1.1×10^{-9}	4.46	23 498.55
	313	1.4×10^{-9}	4.08	19 711.73
	333	1.7×10^{-9}	4.12	16 739.19
	353	2.0×10^{-9}	3.99	14 442.57
	373	2.0×10^{-9}	4.70	12 333.27
Sample 3	298	2.2×10^{-9}	1.97	26 862.74
	313	2.6×10^{-9}	2.00	22 297.33
	333	2.9×10^{-9}	2.01	19 623.74
	353	3.2×10^{-9}	2.00	18 647.26
	373	4.2×10^{-9}	2.29	12 121.30
Sample 4	298	1.7×10^{-9}	2.70	26 266.28
	313	2.2×10^{-9}	2.66	20 120.96
	333	2.4×10^{-9}	2.59	18 670.92
	353	2.6×10^{-9}	2.73	18 158.81
	373	3.4×10^{-9}	2.74	12 521.28

Table 5 Comparison of Henry's constants (dimensionless)

Sample	Sorbate	Temperature (K)	Technique	K (–)	Reference
Sample 3	Propane	313	FRT-ZLC	22 297.33	This work
Sample 3	Propane	333	FRT-ZLC	19 623.74	This work
Sample 3	Propane	353	FRT-ZLC	18 647.26	This work
Sample 3	Propane	373	FRT-ZLC	12 121.30	This work
Zeolite	*n*-Hexane	473	ZLC	7 909.00	(Bárcia et al. 2005)
Beta amino-MIL-53 (Al) (MOF)	*n*-Heptane	453	Pulse chromatography	1087.00	(Couck et al. 2010)
Cerium oxide	*n*-Hexane	523	IG chromatography	17.00	(Díaz et al. 2006)

coates. The experiments were carried out isothermally for three complete dynamic cycles across a temperature range of 25 °C to 100 °C. A mathematical model was developed in Maple to calculate the diffusion coefficients generated from the theoretical ZLC models derived through experimentation. The diffusion coefficients obtained are consistent with previously reported macroscopic data (Granato et al. 2010) and compare well when evaluating the structural differences

Table 6 Overview of diffusivity parameters calculated for different techniques

Gas	Sorbent	E_A (kJ mol^{-1})	Technique	Temperature (K)	D (m^2 s^{-1}) (adsorption)	Reference
Propane	Cordierite monolith	6 ± 2.2	FRT-ZLC	373	2.0×10^{-9}	This study
Propane	Zeolite NaCa-LTA-2	–	PFG-NMR	353	1.5×10^{-11}	(Mehlhorn et al. 2012)
Propane	Silica Mesopore	–	MD Simulations	300	2.0×10^{-8}	(Krishna and van Baten 2011)
Isobutane	Mesoporous glass	–	MD Simulations	300	1.0×10^{-10}	(Fernandes and Gavalas 1999)
Propane	Silicalite-1	6.7	FR	333	5.0×10^{-9}	(Van-Den-Begin et al. 1989)
Propane	Silicalite-1	13.0	ZLC	300	3.5×10^{-11}	(Eic and Ruthven 1989)
Propane	Silicalite-1	25.6	CPC	500	3.0×10^{-9}	(Hufton and Ruthven 1993)
Propane	Silicalite-1	8.0	Wicke-Kallenbach	298–334	5.0×10^{-10}	(Sun et al. 1996a, 1996b)
Propane	ZSM-5	5.0	QENS	300	2.0×10^{-11}	(Jobic et al. 1992)
Propane	NaX zeolite	7.9	PFG-NMR	307	7.0×10^{-10}	(Schwarz et al. 1995)
Propane	13X zeolite	7.9	MD simulations	373	2.9×10^{-9}	(Granato et al. 2010)

of the washcoats of each sample. FRT was also able to successfully compare and contrast the diffusivity differences between ad and desorption transients within the washcoat of monolith samples to shed further light on microporous diffusivity studies.

References

Armenisea, S., Nebraa, M., García-Bordejéa, E., Monzón, A.: Scientific bases for the preparation of heterogeneous catalysts. In: Proceedings of the 10th International Symposium, Louvain-la-Neuve, Belgium, 11–15 July, pp. 11–15. Elsevier, Amsterdam (2010)

Banasa, K., Brandani, F., Ruthven, D., Stallmacha, F., Kärger, J.: Combining macroscopic and microscopic diffusion studies in zeolites using NMR techniques. J. Magn. Reson. Imaging **23**(2), 227–232 (2005)

Bárcia, P., Silva, J., Rodrigues, A.: Adsorption equilibrium and kinetics of branched hexane isomers in pellets of BETA zeolite. Microporous Mesoporous Mater. **79**(1–3), 145–163 (2005)

Boger, T., Heibel, A., Sorensen, C.: Monolithic catalysts for the chemical industry. Ind. Eng. Chem. Res. **2004**(43), 4602–4611 (2004)

Brandani, F.: Ph.D. thesis, University of Maine (2002)

Brandani, S., Hufton, J., Ruthven, D.: Self-diffusion of propane and propylene in 5A and 13X zeolite crystals studied by the tracer ZLC method. Zeolites **15**(7), 624–631 (1995)

Brito, M., Zhu, D., Kriven, W.: Developments in advanced ceramics and composites: a collection of papers presented at the 29th International Conference on Advanced Ceramics and Composites, 23–28 January 2005, Cocoa Beach, Florida (2005)

Buffham, B., Mason, G., Meacham, R.: Sorption-effect chromatography. Journal of Chromatographic Science **24**(6), 265–269 (1986a)

Buffham, B., Mason, G., Meacham, R.: Sorption-effect chromatography. J. Chromatogr. Sci. **24**(6), 265–269 (1986b)

Buffham, B., Mason, G., Meacham, R.: Absolute gas chromatography. Proc. R. Soc. A, Math. Phys. Eng. Sci. **440**(1909), 291–301 (1993)

Buffham, B., Hellgardt, K., Heslop, M., Mason, G.: Remote sensing of the flux responses of a gas–solid catalytic micro-reactor. Chem. Eng. Sci. **55**(9), 1621–1632 (2000)

Cavalcante, C. Jr., Brandani, S., Ruthven, D.: Evaluation of the main diffusion path in zeolites from ZLC desorption curves. Zeolites **18**(4), 282–285 (1997)

Chen, G., Yuan, Q., Li, H., Li, S.: CO selective oxidation in a microchannel reactor for PEM fuel cell. Chem. Eng. J. **101**(2004), 101–106 (2004)

Chmelik, C., Enke, D., Galvosas, P., Gobin, O., Jentys, A., Jobic, H., Kärger, J., Krause, C.B., Kullmann, J., Lercher, J., Naumov, S., Ruthven, D., Titze, T.: Nanoporous glass as a model system for a consistency check of the different techniques of diffusion measurement. Chem. Phys. Chem. **12**, 1130–1134 (2011)

Ciambelli, P., Palma, V., Palo, E.: Comparison of ceramic honeycomb monolith and foam as Ni catalyst carrier for methane autothermal reforming. Catal. Today **155**(1–2), 92–100 (2010)

Couck, S., Rémy, T., Baron, G., Gascon, J., Kapteijn, F., Denayer, J.: A pulse chromatographic study of the adsorption properties of the amino-MIL-53 (al) metal-organic framework. PCCP, Phys. Chem. Chem. Phys. **12**(32), 9413–9418 (2010)

Crank, J.: The Mathematics of Diffusion. Oxford University Press, London (1979)

Díaz, E., de Rivas, B., López-Fonseca, R., Ordóñez, S., Gutiérrez-Ortiz, J.: Characterization of ceria-zirconia mixed oxides as catalysts for the combustion of volatile organic compounds using inverse gas chromatography. J. Chromatogr. A **1116**(1–2), 230–239 (2006)

Eic, M., Ruthven, D.: Diffusion of linear paraffins and cyclohexane in NaX and 5A zeolite crystals. Zeolites **8**(6), 472–479 (1988)

Eic, M., Ruthven, D.: Intracrystalline diffusion of linear paraffins and benzene in silicalite studied by the ZLC method. Stud. Surf. Sci. Catal. **49**, 897–905 (1989)

Fernandes, N., Gavalas, G.: Molecular dynamics simulations of diffusion in mesoporous glass. Ind. Eng. Chem. Res. **38**(3), 723–730 (1999)

García-Sánchez, A., van den Bergh, J., Castillo, J., Calero, S., Kapteijn, F., Vlugt, T.: Influence of force field parameters on computed diffusion coefficients of CO_2 in LTA-type zeolite. Microporous Mesoporous Mater. **158**, 64–76 (2012)

Gobin, O.: Seminar thesis, Laval University (2006)

Gonzo, E., Gottifredi, J.: Heat and mass transfer limitations in monolith reactor simulation with non uniform washcoat thickness. Lat. Am. Appl. Res. **40**(1), 15–21 (2010)

Granato, M., Jorge, M., Vlugt, T., Rodrigues, A.: Diffusion of propane, propylene and isobutane in 13X zeolite by molecular dynamics. Chem. Eng. Sci. **65**(9), 2656–2663 (2010)

Guimarães, A., Möller, A., Staudt, R., de Azevedo, D., Lucena, S., Cavalcante, C.: Diffusion of linear paraffins in silicalite studied by the ZLC method in the presence of CO_2. Adsorption **16**(1–2), 29–36 (2010)

Gunadi, A., Brandani, S.: Diffusion of linear paraffins in NaCaA studied by the ZLC method. Microporous Mesoporous Mater. **90**(1–3), 278–283 (2006)

Heck, R., Farrauto, R., Gulati, S.: Catalytic air pollution control: commercial technology. Platin. Met. Rev. **54**(3), 180–183 (2010)

Heck, R., Gulati, S., Farrauto, R.: The application of monoliths for gas phase catalytic reactions. Chem. Eng. J. **82**(1–3), 149–156 (2001)

Hufton, J., Ruthven, D.: Diffusion of light alkanes in silicalite studied by the zero length column method. Ind. Eng. Chem. Res. **32**(10), 2379–2386 (1993)

James, A., Brindley, J., McIntosh, A.: Multi-channel monolith reactors as dynamical systems. Combust. Flame **134**(2003), 193–205 (2003)

Jobic, H., Bée, M., Kearley, G.: Dynamics of ethane and propane in zeolite ZSM-5 studied by quasi-elastic neutron scattering. Zeolites **12**(2), 146–151 (1992)

Karge, H., Weitkamp, J., Brandani, S.: Adsorption and Diffusion (2008)

Karger, J., Ruthven, D.: Diffusion in Zeolites and Other Micro-porous Solids (1992)

Koci, P., Štěpánek, F., Kubíček, M., Marek, M.: Modelling of micro/nano-scale concentration and temperature gradients in porous supported catalysts. Chem. Eng. Sci. **62**(18–20), 5380–5385 (2007)

Krishna, R., van Baten, J.: Influence of adsorption on the diffusion selectivity for mixture permeation across mesoporous membranes. J. Membr. Sci. **369**(1–2), 545–549 (2011)

Kärger, J.: The beauty of the different views on diffusion. Defect Diffus. Forum **326–328**, 1–11 (2012)

Loos, J.: Improved estimation of zeolite diffusion coefficients from zero-length column experiments. Chem. Eng. Sci. **55**(1), 51–65 (2000)

Mason, G.: Capillary viscometry by perturbation of flow and composition. Chem. Eng. Sci. **53**(15), 2665–2674 (1998)

Mehlhorn, D., Valiullin, R., Kärger, J., Cho, K., Ryoo, R.: Exploring mass transfer in mesoporous zeolites by NMR diffusometry. Materials **5**, 699–720 (2012)

More, H., Hayes, R., Liu, B., Votsmeier, M., Checkel, M.: The effect of catalytic washcoat geometry on light-off monolith reactors. Top. Catal. **37**(2–4), 155–159 (2006)

Palmer, C., Sasegbon, A., Hellgardt, K.: In situ measurement of gas adsorption processes using flux response technology. Adsorption **17**(5), 783–794 (2011)

Plummer, H., Baird, R., Hammerle, R., Adamczyk, A., Pakko, J.: Measurement of automotive catalyst washcoat loading parameters by microscopy techniques. Microscopy and Microanalysis (2003)

Ranke, W., Joseph, Y.: Determination of adsorption energies and kinetic parameters by isosteric methods. ChemPhysChem **4**(12), 2483–2498 (2002)

Richardson, D., Hellgardt, K., Russell, P., Mason, G., Buffham, B.: A study of ammonia decomposition over Pt/Alumina preparation of catalyst. Chem. Eng. **82**, 1397–1403 (2004)

Richardson, D., Mason, G., Buffham, B., Hellgardt, K., Cumming, I., Russell, P.: Viscosity of binary mixtures of carbon monoxide and helium. J. Chem. Eng. Data **53**(1), 303–306 (2008)

Russell, P., Buffhama, B., Mason, G., Heslop, M.: Perturbation viscometer to measure the viscosity gradients of gas mixtures. AIChE J. **49**(8), 1986–1994 (2003)

Russell, P., Buffhama, B., Mason, G., Heslop, M.: Perturbation viscometry of gas mixtures: fitting a model to logarithmic viscosity gradients. Chem. Eng. Sci. **57**(21), 4493–4504 (2002)

Ruthven, D.: Introduction to Zeolite Science and Practice. Elsevier, Amsterdam (2001)

Ruthven, D., Brandani, S.: Measurement of diffusion in porous solids by zero length column (ZLC) methods. Membr. Sci. Technol. **6**, 187–212 (2000)

Ruthven, D., Heinke, L., Kärger, J.: Sorption kinetics for surface resistance controlled systems. Microporous Mesoporous Mater. **132**(1–2), 94–102 (2010)

Schwarz, H., Ernst, H., Ernst, S., Kärger, J., Röser, T., Snurr, R., Weitkamp, J.: NMR study of intrinsic diffusion and reaction in CsNaX type zeolites. Appl. Catal. A, Gen. **130**(2), 227–241 (1995)

Silva, J.: Analysis of ZLC technique for diffusivity measurements in bidisperse porous adsorbent pellets. Gas Sep. Purif. **10**(4), 207–224 (1996)

Sun, M., Talu, O., Shah, D.: Adsorption equilibria of C 5–C 10 normal alkanes in silicalite crystals. J. Phys. Chem. **100**(43), 17276–17280 (1996a)

Sun, M., Talu, O., Shah, D.: Diffusion measurements through embedded zeolite crystals. AIChE J. **42**(11), 3001–3007 (1996b)

Tomašić, V.: Application of the monoliths in DeNOx catalysis. Catal. Today **119**(1–4), 106–113 (2007)

Van-Den-Begin, N., Rees, L., Caro, J., Bülow, M.: Fast adsorption-desorption kinetics of hydrocarbons in silicalite-1 by the single-step frequency response method. Zeolites **9**(4), 287–292 (1989)

Zhang, F., Hayes, R., Kolaczkowski, S.: A new technique to measure the effective diffusivity in a catalytic monolith washcoat. Chem. Eng. Res. Des. **82**(4), 481–489 (2004)